Talanta 300 (2026) 129227

Contents lists available at ScienceDirect

Talanta

journal homepage: www.elsevier.com/locate/talanta

Site-specific conjugated antibody-element tags for single-cell ICP-MS

Haowen Hu [a,1], Zhengxian Lv [a,c,1], Yixin Guo [a], Li Yi [a], Limin Yang [a], Xiaowen Yan [a,b,*], Qiuquan Wang [a,**]

[a] Department of Chemistry and the MOE Key Laboratory of Spectrochemical Analysis & Instrumentation, College of Chemistry and Chemical Engineering, Xiamen University, Xiamen, 361005, China
[b] Innovation Laboratory for Sciences and Technologies of Energy Materials of Fujian Province (IKKEM), Xiamen, 361005, China
[c] Zhejiang Key Laboratory of Environment and Health of New Pollutants, School of Environment, Hangzhou Institute for Advanced Study, University of Chinese Academy of Sciences, Hangzhou, 310024, China

ARTICLE INFO

Keywords:
Site-specific antibody conjugation
Antibody elemental tag
ICP-MS
Single-cell analysis
Tumor biomarker

ABSTRACT

Inductively coupled plasma mass spectrometry (ICP-MS) has demonstrated high sensitivity, accuracy, and multi-element detection capacity for biomolecule analysis. However, traditional ICP-MS-used antibody-elemental tags (AETs) are typically constructed through random antibody modification, resulting in structural heterogeneity that compromises binding affinity, specificity, and analytical performance. To overcome this limitation, we developed a traceless, site-specific conjugation strategy that enables precise attachment of a single-stranded DNA (ssDNA) to the K248 residue of IgG antibodies. The "traceless" feature ensures that no residual peptide remains on the antibody after labeling, thereby preserving its native structure and binding activity. The ssDNA serves as a bridge for hybridization with europium (Eu)-loaded MS2 capsid nanoparticles, which act as signal amplifiers by delivering a large payload of metal atoms. Through the integration of precise antibody modification and high-capacity MS2 elemental carriers, the resulting **site-specific** AETs (ssAETs) exhibit exceptional structural uniformity, stability, and sensitivity. Using human epidermal growth factor receptor 2 (HER2) as a model, the AETs synthesized through our strategy demonstrated exceptional specificity and quantitative performance, achieving 1.8-fold stronger single-cell signals and labeling 1.5 times more HER2-positive cells compared with randomly conjugated antibodies. This traceless, site-specific ssAET platform offers a versatile and precise approach for highly sensitive and quantitative single-cell bioanalysis using ICP-MS.

1. Introduction

Recently, inductively coupled plasma mass spectrometry (ICP-MS) has emerged as a powerful bioanalytical tool in biomedical research due to not only its exceptional sensitivity, wide dynamic range, and strong resistance to matrix interference, but also the developments of elemental tags and their labeling strategies [1–12]. Among them, antibody-elemental tags (AETs) serve as important molecular bridges between biological recognition events and elemental signal output [13,14]. By converting the specific binding of antibodies to their target antigens into measurable metal signals, AETs allow ICP-MS to bypass limitations associated with the different signal response of different chemical form of the analyte, enabling accurate and highly sensitive quantification. Building on this capability, efforts have increasingly focused on improving elemental tag design. In 2001, Zhang's group first reported europium isotope-labeled AETs [1], establishing the feasibility of integrating immunoassays with elemental mass spectrometry for biomolecular analysis. As the demand for higher sensitivity increased, particularly in single-cell applications, subsequent research focused on optimizing metal-rich reporter units to maximize signal output. In 2007 and 2009, Winnik and co-workers developed two types of lanthanide-containing polymer AETs [15,16], markedly increasing the number of metal atoms per tag and thereby enhancing detection sensitivity. Building on these advances, in 2019, Wang's group first reported

This article is part of a special issue entitled: SC/SP approaches for ICP-MS published in Talanta.

* Corresponding author. Department of Chemistry and the MOE Key Laboratory of Spectrochemical Analysis & Instrumentation, College of Chemistry and Chemical Engineering, Xiamen University, Xiamen 361005, China.
** Corresponding author.
E-mail addresses: xwyan@xmu.edu.cn (X. Yan), qqwang@xmu.edu.cn (Q. Wang).
[1] H.H. and Z.L. contributed equally.

https://doi.org/10.1016/j.talanta.2025.129227
Received 25 August 2025; Received in revised form 15 October 2025; Accepted 5 December 2025
Available online 6 December 2025
0039-9140/

a virus-like Ln–MS2 signal amplifier capable of incorporating over one thousand of lanthanide atoms per MS2 capsid, achieving three orders of magnitude signal amplification [17] and providing a robust platform for ultrasensitive bioanalysis. In parallel, other strategies, including the use of noble metal nanoparticles [18,19] and metal-doped nanoparticles [20–22], have also been explored to further improve sensitivity, enabling reliable detection of low-abundance targets such as cell surface proteins, bacteria, and circulating vesicles.

However, despite significant advances in the development of elemental reporters, less attention has been paid to the recognition component, i.e. Antibodies, and to their conjugation strategies with elemental tags. Currently, most AETs are still constructed via non-selective chemical conjugation strategies, typically involving the reaction of surface-exposed lysine or cysteine residues with activated functional groups on the elemental tag [12,15–23]. While operationally straightforward, this random conjugation approach presents two major limitations. First, the lack of control on conjugation sites and stoichiometry can result in modification of residues within or near the antigen-binding regions (paratopes), potentially reducing the antibody's binding affinity and target specificity [24–26]. Second, the resulting conjugation heterogeneity leads to batch-to-batch variability, poor reproducibility, and compromised signal consistency [27]. These issues are particularly detrimental in applications that demand high analytical precision, such as single-cell analysis, spatial proteomics, or absolute quantification, where uniform signal output and reliable biomolecular recognition are critical. Moreover, the unpredictability in metal-to-antibody ratio hinders quantitative interpretation of elemental signals, ultimately limiting the broader utility of AETs in high-resolution or multiplexed bioanalytical.

To overcome the limitations of unspecific antibody conjugation, various methods have been developed to direct the conjugation to specific locations on the antibody, including enzymatic methods [28] (e.g., using microbial transglutaminase or sortase A), Thiomab engineering [29] (introducing reactive cysteines at defined positions), and the incorporation of non-natural amino acids [30] (bearing orthogonal chemical handles). While effective, these techniques typically require complex, genetic manipulation, antibody re-engineering, making them technically challenging and costly [31]. Recently, peptide-mediated affinity labeling technology represents a method that employs peptides as bridges to specifically bind labels to target biomolecules, such as proteins, nucleic acids, and cell surface receptors. Ito et al. [32] reported a 17-amino-acid Fc-binding peptide (GPDCAYHKGELVWCTFH) that selectively recognizes the Fc region of human IgG and delivers an NHS ester functional group specifically to lysine 248. This strategy achieved site-specific modification with nanomolar binding affinity (Kd = 10 nM) and demonstrated high selectivity toward therapeutic antibodies such as trastuzumab. Despite these advantages, the peptide remains on the antibody after conjugation, which may sterically hinder interactions with Fc receptors or effector molecules. Therefore, there is a compelling need for a highly specific antibody coupling strategy with minimal structural interference to construct next-generation AETs.

In this work, using trastuzumab (a therapeutic anti-HER2 IgG) as a model antibody, we report the construction of uniform, stable, and highly sensitive antibody–elemental tags (AETs) through a traceless, site-specific conjugation strategy, where the labeling proceeds via a cleavable intermediate that leaves no residual peptide or linker on the antibody, thus preserving its native structure for accurate single-cell ICP-MS (SC-ICP-MS) analysis (Scheme 1). The strategy comprises three steps: (1) a rationally designed Fc-targeted acyl transfer reagent (FTA), consisting of an Fc-binding peptide, thioester linker, and azide payload, binds to the Fc region and delivers the azide specifically to lysine 248 (K248) via a proximity-induced acyl transfer reaction, accompanied by self-release of the peptide ligand, generating site-specific azide-labeled antibodies (ssAAb); (2) the ssAAb is subsequently reacted with DBCO-modified DNA oligonucleotides via strain-promoted azide–alkyne cycloaddition (SPAAC), forming uniform DNA-functionalized antibodies (ssDAb); (3) finally, europium (Eu)-loaded MS2 phage capsid nanoparticles [16] which serve as signal amplifiers by delivering a large payload of metal atoms, are hybridized with complementary DNA-bearing ssDAb to form the complete AET construct (ssAET). This modular AETs construction strategy offers precise stoichiometric control, minimal structural perturbation, and robust signal amplification, providing a powerful tool for ultrasensitive and reproducible ICP-MS-based single-cell analysis. The cellular labeling effects of the elemental tag prepared using both traceless site-specific conjugation strategy and random conjugation strategy were assessed in different

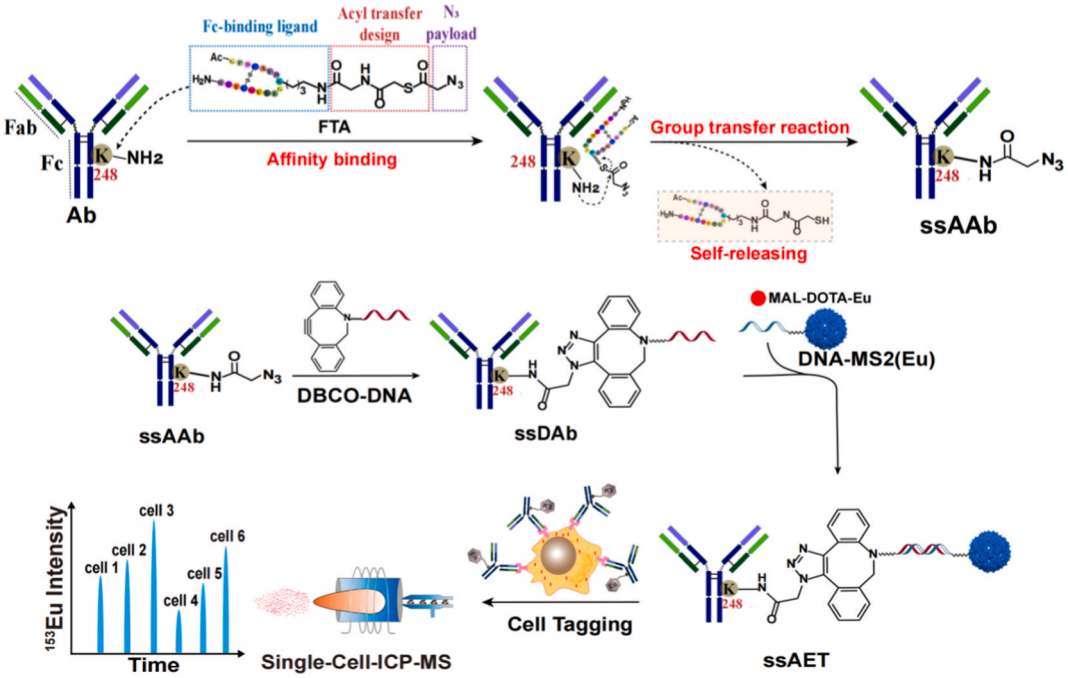

Scheme 1. Diagram of Building Up ssAET for SC-ICP-MS-Based Immunoassay.

breast cancer cell models with different levels of HER2 protein (MDA-MB-231, SKBR-3) to demonstrate high specificity, affinity, and homogeneity of the ssAET.

2. Experimental SECTION

Chemicals and Reagents. All reagents were of analytical grade or higher and used as received. 2-(Tritylthio)acetic acid was obtained from Bide Pharmatech (Shanghai, China). NHS, EDC, HATU, and SMCC were purchased from Energy Chemical (Shanghai, China). The Fc-binding peptide, glycine, oligonucleotides, Traut's reagent (2-iminothiolane hydrochloride, purity >98 %), and SDS-PAGE preparation kit were synthesized by Sangon Biotech (Shanghai, China). DIPEA and Maleimide-PEG2k-NHS were purchased from Aladdin (Shanghai, China). Triethylsilane and azidoacetic acid NHS ester were purchased from Titan Scientific (Shanghai, China). Trastuzumab was purchased from Roche (Shanghai, China). Centrifugal filters were obtained from Millipore Corp (Billerica, MA, USA) and PALL (Beijing, China). IdeS protease was purchased from MedChem Express (Monmouth Junction, NJ, USA). SDS-PAGE loading buffer (5 × , with DTT) was obtained from Solarbio (Beijing, China). Europium standard solution (1 μg/mL) was purchased from the National Analysis and Testing Center for Nonferrous Metals & Electronic Materials (Beijing, China). Lanthanide-doped polystyrene beads (Ln-PS, 3 μm, Ln = Ce, Eu, Ho, Lu) were obtained from Fluidigm (California, USA). Mal-DOTA was purchased from Macrocyclics (Dallas, TX, USA). Eu(NO3)3 was purchased from Yunshan Biochemical Technology (Guangzhou, China). MS2 bacteriophage strain 15597-B1 was acquired from ATCC (Manassas, USA). Human breast cancer cell lines MDA-MB-231 (HER2 negative) and SKBR-3 (HER2 positive) were obtained from the Cell Bank of the Chinese Academy of Sciences (Shanghai, China). Other biological reagents, including NuPAGE™ LDS buffer, SYBR™ Gold nucleic acid gel stain, DMEM, heat-inactivated FBS, and penicillin-streptomycin, were from Thermo Fisher Scientific (Waltham, MA, USA). Unless otherwise noted, general chemicals and solvents were purchased from Sinopharm Chemical Reagent Co. (Shanghai, China).

Instruments. The number of Eu atoms tagged on one MS2 particle in the elemental tag was determined by HPLC/^{153}Eu-species-unspecific isotope dilution ICP-MS. Before ICP-MS(A NEXION 2000 ICPMS, PerkinElmer, SCIEX, Canada), separation of the sample was carried out on an LC-20AD LC system (Shimadzu, Kyoto, Japan) with a size exclusion chromatography column (SEC, Waters Xbridge Protein BEH 4.6 I.D. × 300 mm in length, 2.5 μm particle size). An 0.25 mL min^{-1} flow rate and 100 % 25 mM NH_4Ac (isocratic elution) were applied. The effluent from the column (0.25 mL min^{-1}) was mixed with the enriched ^{153}Eu standard solution (0.06 mL min^{-1}, 10 μg/L) by a syringe pump (Cole-Parmer, East Bunker Court Vernon Hills, IL) via a three-way connection and continuously pumped into ICP-MS. The online isotope ratio of ^{151}Eu to ^{153}Eu was monitored using ICP-MS equipped with a concentric pneumatic nebulizer and a cyclonic spray chamber. The calculation of transforming ^{151}Eu and ^{153}Eu isotope chromatograms into Eu mass flow chromatograms was determined by the following online isotope dilution equation:

$$MF_{sample}(t) = MF_{spike}\frac{153}{151}\frac{\left(A^{151}_{spike} - A^{153}_{spike}R_{sample}(t)\right)}{\left(A^{153}_{sample}R_{sample}(t) - A^{151}_{spike}\right)}$$

where MF_{sample} and MF_{spike} denote the mass flow of Eu in the sample and spiked solution. M_{sample} and M_{spike} denote the atomic mass of Eu in the sample and spike solution, and A^{151}_{sample} and A^{151}_{spike} denote the isotope abundance of ^{151}Eu in the sample and spike solution. A^{153}_{sample} and A^{153}_{spike} denote the isotope abundance of ^{153}Eu in the sample and spike solution. $R_{sample}(t)$ is the online measured ^{151}Eu/^{153}Eu isotope ratio during HPLC/ICP-MS. Then, the chromatogram of isotope ratios is transformed into the chromatogram of mass flow (mass vs time) using the isotope dilution equation. The absolute amount of Eu in different species can be obtained by integrating the corresponding peaks in the chromatogram of mass flow. The ICP-MS operational parameters are listed in Table S1.

Single-cell analysis was conducted using a home-made oil-free passive microfluidic device (OFPMS) [33] for single-cell injection under the optimized conditions listed in Table S2. The transport efficiency (95.4 ± 2.8 %) was determined by the particle frequency method [34], based on the number of detected ^{153}Eu events from Ln-doped beads at a known concentration of 1 × 10^5 particles/mL.

Synthesis of FcBP-TE-Az (FTA). To generate (2-(tritylthio)acetyl) glycine (S1), 2-(tritylthio)acetic acid (334 mg, 1 mmol) was dissolved in 2.0 mL of DMF. NHS (138 mg, 1.2 mmol) and EDC (230 mg, 1.2 mmol) were added and the reaction mixture was stirred overnight at room temperature. The mixture was then slowly added to a glycine solution (112.5 mg, 1.5 mmol) in DMF:2 × PBS = 1:1 (200 mL) and stirred for 3 h. Solvent was removed by rotary evaporation, extracted with dichloromethane using ultrasound, filtered, and purified by silica gel chromatography (dichloromethane:methanol = 20:1 with 0.3 % acetic acid). The resulting compound S1 (20 mM) was reacted with HATU (10 mM), DIPEA (15 mM), and FcBP (5 mM) in DMF for 1 h to obtain P1, which was purified by semi-preparative HPLC (LC-16P, Shimadzu, Kyoto, Japan). Next, P1 was dissolved in DCM (700 μL), cooled to 0 °C, and treated with TFA (630 μL) and triethylsilane (70 μL) for 1 h. The reaction mixture was concentrated and the crude product was purified to yield P2. Finally, P2 (6 mM) was reacted with Az-NHS ester (6 mM) in DMF/2 × PBS = 1:1 for 15 min and the resulting FTA was purified by semi-preparative HPLC.

Preparation of Site-Specific ssAET. Excess FTA was removed by 100 kDa MWCO spin filtration. ssAAb was reacted with DBCO-DNA (40 eq) at 37 °C overnight. Eu(NO_3)$_3$ (500 mM in 2 % HNO_3) was mixed with Mal-DOTA (in CH_3COONH_4, pH 6.8) at a 1:2 M ratio for 3 h, then purified by HPLC. MS2 capsid proteins (100 μM monomer) were treated with Traut's reagent in $NaHCO_3$ buffer (pH 8.0) for 5 h to generate MS2-SH, followed by filtration. For dual labeling, MS2-SH was first reacted with DBCO-DNA (3 eq) in HEPES (25 mM, pH 7.2) for 2 h, then with Mal-DOTA-Eu (50 eq) for 6 h. After purification, ssDAb was hybridized with DNA-MS2(Eu) at a 2:1 ratio in HEPES buffer containing 8.5 g/L NaCl (pH 7.2) for 30 min and stored at 4 °C.

Preparation of Random-Conjugated Antibody Elemental Tag (rcAET). Trastuzumab (5 mg/mL) was reacted with Maleimide-PEG$_{2k}$-NHS (10 eq) in PBS (pH 7.2, 5 % DMF) at 37 °C for 3 h. Excess reagent was removed by 30 kDa MWCO spin filtration. The resulting MAL-antibody was reacted with MS2-SH (5:1 ratio) for 3 h, followed by Mal-DOTA-Eu (50 eq) for 6 h. The final rcAET was purified and stored at 4 °C.

Cell Culture. SKBR-3 and MDA-MB-231 cells were cultured in DMEM supplemented with 10 % heat-inactivated FBS and 100 U/mL penicillin-streptomycin at 37 °C in a 5 % CO_2 humidified incubator. Cell viability and counts were assessed using 0.4 % trypan blue.

Cell Tagging and Fixation. Cells were washed with 25 mM HEPES buffer (pH 7.2), trypsinized for 3 min, neutralized with culture medium, and resuspended in binding buffer (HEPES + 8.5 g/L NaCl + 1 % FBS) to 10^6 cells/mL. 100 μL aliquots (10^5 cells) were incubated with ssAET or rcAET (53 nM) for 1 h on ice to inhibit endocytosis. After labeling, cells were fixed with 4 % paraformaldehyde for 15 min, washed twice, resuspended in 10 mM NH_4HCO_3, and filtered through a 300-mesh nylon screen for SC-ICP-MS analysis.

Data Processing. Time-resolved ICP-MS data were processed by first calculating the overall signal mean and standard deviation (SD). A threshold defined as mean + 5 × SD was then applied to identify individual cell events. Any continuous sequence of data points exceeding this threshold was considered one cell-derived signal event (i.e., an individual cell's ion cloud). For each such event, all consecutive data points above the threshold are summed to obtain the total integrated ^{153}Eu intensity corresponding to that single cell.

3. Results and discussion

3.1. Generation and characterization of ssAET

Although traceless site-specific conjugation was originally developed for antibody–drug conjugates (ADCs) [35–37], its application in AET construction represents a novel extension. Here, we employed an Fc-binding peptide (FcBP) [32] to direct a thioester-linked azidoacetyl group specifically to K248 on the Fc region. Upon binding, a proximity-driven acyl transfer installs the azide moiety via stable amide formation, while the FcBP is spontaneously released. This strategy yields a cleanly modified antibody with precise stoichiometry and no residual linker, enabling modular DNA coupling and subsequent assembly with metal-loaded nanostructures.

To validate the functionality of the acyl transfer reagent, we synthesized the FTA reagent following the scheme shown in Scheme S1. All synthetic intermediates (S1, P1, P2, and the final FTA product) were fully characterized by RP-HPLC-UV, ESI-MS, ^{1}H NMR, ^{13}C NMR, and MALDI-TOF-MS (Fig. S1–S5). As shown in Fig. 1a, the azide group was successfully introduced onto the K248 side chain of trastuzumab via the FcBP-guided acyl transfer using the flexible 2-azidoacetyl thioester moiety. Reaction conditions were optimized by varying the equivalents of FTA (12, 20, and 40 equivalents).

To assess the site specificity of the azide modification, the ssAAb was digested with IdeS, which cleaves the IgG hinge region and separates the Fab and Fc fragments [38]. NanoLC-MS analysis showed that the Fc fragment of the modified antibody exhibited a mass increase of +83 Da (MW 23,522) compared to the unmodified Fc (MW 23,439), consistent with a single azidoacetyl modification at K248 (Fig. S6), confirming the successful site-specific acyl transfer. Optimization studies revealed that a molar ratio of 1:20 (antibody: FTA) was sufficient to achieve near-quantitative modification.

To enable downstream functionalization, ssAAb was conjugated with DBCO-DNA through strain-promoted azide-alkyne cycloaddition (SPAAC) using 40 equivalents of DBCO-DNA, resulting in the formation of ssDAb. To verify the homogeneity and fragment-selectivity of DNA conjugation, the products were analyzed by 10 % SDS-PAGE following IdeS digestion, with Coomassie and SYBR Gold staining (Fig. 1b). The gel analysis confirmed that DNA was conjugated specifically to the Fc, not the Fab, region of the antibody, with a near 1:1 stoichiometry, as determined by grey value quantification. The resulting ssDAb provides a standardized molecular interface for subsequent hybridization with metal-loaded DNA nanostructures for AET assembly.

Previous work in our laboratory has demonstrated the viruslike Ln-MS2 signal-amplifier could carry hundreds of Ln atoms on each MS2 capsid, and enable nearly three orders of magnitude signal-amplification [14]. Here, we employed MS2 virus-like particles as Eu carriers to construct signal-amplifying ssAET. To introduce functional groups for dual labeling, MS2 capsid proteins were thiolated using Traut's reagent, converting amines on both interior and exterior surfaces to thiols. MALDI-TOF-MS analysis confirmed conversion of six out of seven reactive amines per monomer (Fig. S7). Cysteine-modified MS2 was then reacted with a small amount of MAL-DNA linker followed by a high excess of MAL-DOTA-Eu to construct the elemental tag DNA-MS2(Eu).

The conjugates were validated by 15 % SDS-PAGE (Fig. S8), and the Eu content per particle was determined via ^{153}Eu species-unspecific isotope dilution ICP-MS (SUID-ICP-MS) [39] coupled with size-exclusion chromatography (SEC) (Fig. S9). To determine the optimal assembly ratio for hybridization, ssDAb and DNA-MS2(Eu) were mixed in 25 mM HEPES (pH 7.2) at various molar ratios (0.5:1, 1:1, 1.5:1, 2:1, and 5:1) using complementary oligonucleotide sequences (Fig. 2a). SEC traces showed a gradual increase in peak area up to 2:1 ssDAb:MS2-Eu ratio, beyond which no further increase was observed (Fig. 2b). Statistical analysis ($P = 0.9149$, ns) confirmed 2:1 as the saturation point (Fig. 2c). The final hybrid product (ssAET) exhibited uniform electrophoretic migration on 1 % agarose gel, confirming its homogeneity (Fig. 2d). Collectively, these results demonstrate that the traceless conjugation strategy enables precise construction of homogeneous ssAETs with well-defined stoichiometry and modular compatibility for downstream elemental labeling and detection.

3.2. Optimization of ssAET tagging concentration

To enable ssAET to achieve saturated labeling of the HER2 receptor on the cell surface, the concentration of ssAET needs to be optimized. For this purpose, different concentrations of ssAET were introduced into SK-BR3, and subsequently, the Eu mass per cell was quantified through SC-ICP-MS analysis. For such quantification, the SC-ICP-MS was

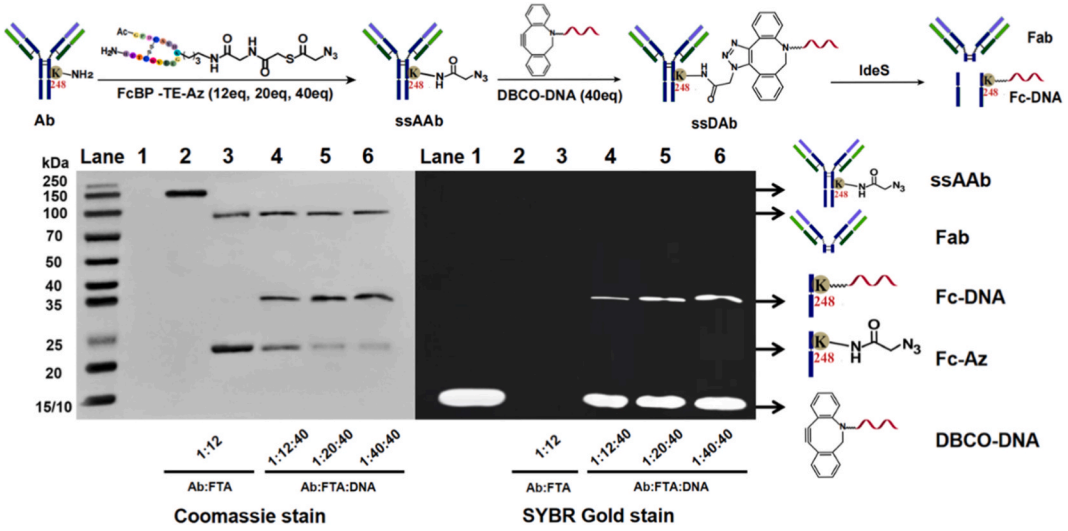

Fig. 1. Generation of ssDAb. (a) General synthetic scheme of ssDAb. First, Azide was site-specifically attached to Trastuzumab via acyl transfer of FTA at ratios of 12:1, 20:1, and 40:1. The resulting ssAAb was then incubated with identical concentrations of DBCO-DNA via SPAAC reaction. (b) Modification site analysis of ssDAb. SDS-PAGE (10 %) characterizing the conjugation products of ssDAb with varying Ab: FTA ratios. Lane 1 shows the molecular weight of DBCO-DNA at ~10 KDa; Lane 2 shows the complete ssAAb; Lane 3 shows the ssAAb was treated with IdeS to get Fab and Fc-Az domains; At the identical concentration of DBCO-DNA, the ratios of Ab to FTA in lanes 4–6 were 1:12, 1:20, 1:40 respectively and treated with IdeS. 10 % SDS-PAGE was stained with SYBR Gold and Coomassie blue to visualize protein and DNA, respectively. (For interpretation of the references to colour in this figure legend, the reader is referred to the Web version of this article.)

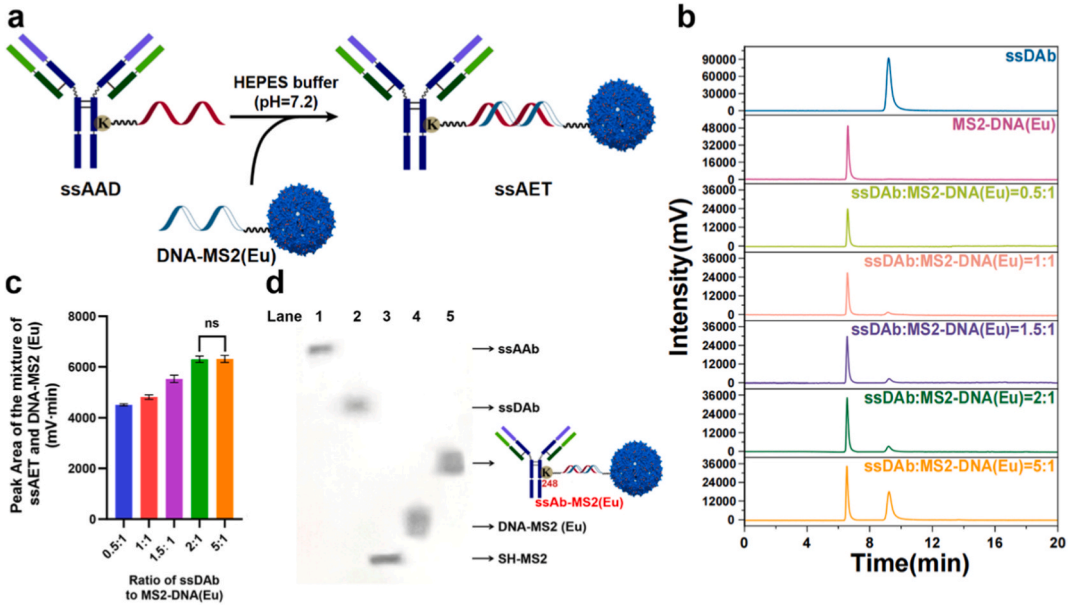

Fig. 2. Generation of ssAET. (a) General synthetic scheme of ssAET. ssDAb and DNA-MS2 (Eu) hybridize in 25 mM HEPES buffer (pH = 7.2) for 30 min using oligonucleotides with complementary sequences at ratios of 0.5:1, 1:1, 1.5:1, 2:1, and 5:1, respectively. (b) SEC analysis of the hybridization situations of ssDAb and DNA-MS2(Eu) at different ratios of 0.5:1, 1:1, 1.5:1, 2:1, and 5:1. The retention time of DNA-MS2(Eu) and ssAET were 6.5 min due to the resolution of the chromatography column, while the retention time of Ab-DNA was 9.1 min. (c) Determination of the ratio of ssDAb to DNA-MS2(Eu) via the peak area of the mixture of ssAET and DNA-MS2(Eu) under different reacting ratios. (d) 1 % agarose gel electrophoresis characterization of ssAET using 2 equiv of ssDAb to the DNA-MS2(Eu). Lane 1 shows the ssAAb; Lane 2 shows the ssDAb; Lane 3 shows the MS2-SH; Lane 4 shows the DNA-MS2(Eu); Lane 5 shows the ssAET.

calibrated using Eu inorganic standards. The signal response per concentration unit was transformed into the mass of Eu per cell using the previously established equation (the previously established Standard solution curve of ^{153}Eu under SC-ICP-MS (Fig. S10) [34]. To select the ssAET concentration, we considered the data obtained in previously published work [6]. We chose 26 nM, 53 nM, and 80 nM of ssAET and rcAET respectively for the labeling of SK-BR3 cells. In the case of HER2-positive SKBR-3 cells, the mass of Eu on each cell increased along with the increase in the concentration of antibody-elemental tag cell labeling, and remained constant when the labeling concentration exceeded 53 nM (Fig. S11). Thus, a concentration of 53 nM of the antibody-elemental tag is sufficient for achieving the saturation labeling of HER2 receptors on the surface of positive cells.

3.3. Evaluation of non-specific adsorption of MS2-Eu elemental carrier

To exclude the possibility that the elemental carrier MS2-Eu itself contributes to background signal through non-specific adsorption, we conducted a control experiment using two breast cancer cell lines with distinct HER2 expression profiles: SK-BR-3 (HER2-positive) and MDA-MB-231 (HER2-negative). Both cell lines were incubated with 53 nM MS2-Eu under the same labeling conditions used for ssAET, but without antibody attachment. The resulting SC-ICP-MS data revealed that the ^{153}Eu signal intensity for both cell types was indistinguishable from that of the blank control (Fig. S12), with no significant high-intensity events detected. This indicates that MS2-Eu nanoparticles do not adsorb non-specifically to the cell membrane under the applied labeling conditions. These findings confirm that the Eu signals observed in subsequent experiments originate from specific antibody–antigen interactions, rather than from passive adsorption of the elemental reporter.

3.4. Comparative evaluation of site-specific and randomly conjugated AETs

To evaluate the differences between AETs generated via traceless site-specific conjugation (ssAET) and those prepared via conventional random conjugation (rcAET), we synthesized rcAET by randomly modifying trastuzumab with MAL-PEG2k-NHS followed by reaction with SH-MS2. As shown in Fig. S13a, rcAET exhibited notable heterogeneity in 8 % SDS-PAGE analysis. Moreover, SEC-SUID-ICP-MS quantification revealed that rcAET carried fewer Eu atoms per MS2 compared to ssAET (Fig. S13b), likely due to inconsistent antibody loading and variable conjugation efficiency. These results suggest that the random strategy compromises elemental density and molecular uniformity of the tag.

We next systematically assessed the labeling performance of both AET formats in detecting HER2 expression on single cells using SC-ICP-MS. The two breast cancer cell lines, HER2-negative MDA-MB-231 and HER2-positive SKBR-3, were labeled with either rcAET or ssAET under optimized conditions (53 nM). The detection efficacy of HER2 receptors by two different strategies-prepared antibody-elemental tags was systematically evaluated from several aspects, including the labeling ability at the single-cell level, the ability to analyze the heterogeneity of HER2 receptors on the surface of the same type of cells, and the cell typing ability.

To evaluate the specificity of the antibody elemental tags constructed based on different strategies in the analysis of cancer cells, MDA-MB-231 and SK-BR3 cells were respectively labeled with rcAET and ssAET. The original signals obtained by SC-ICP-MS are shown in Fig. S14. Following the processing of the original data, the average 153Eu signal intensity was calculated, and a frequency distribution histogram of 153Eu content across individual cells was generated to assess the heterogeneity of HER2 receptor expression within the same cell type. As shown in Fig. 3a, the ^{153}Eu signal intensity on SKBR-3 cells was significantly higher than that on MDA-MB-231 for both AETs ($p < 0.0001$), confirming the target specificity of each tag. Notably, ssAET produced a 1.8-fold higher signal and labeled 1.5 times more SKBR-3 cells compared to rcAET, indicating an enhanced labeling efficiency and detection sensitivity. This improvement likely stems from the homogeneity and preserved antigen-binding functionality of the site-specifically conjugated antibody.

To further explore their ability to reveal expression heterogeneity of HER2 receptors, we analyzed the distribution of ^{153}Eu content among

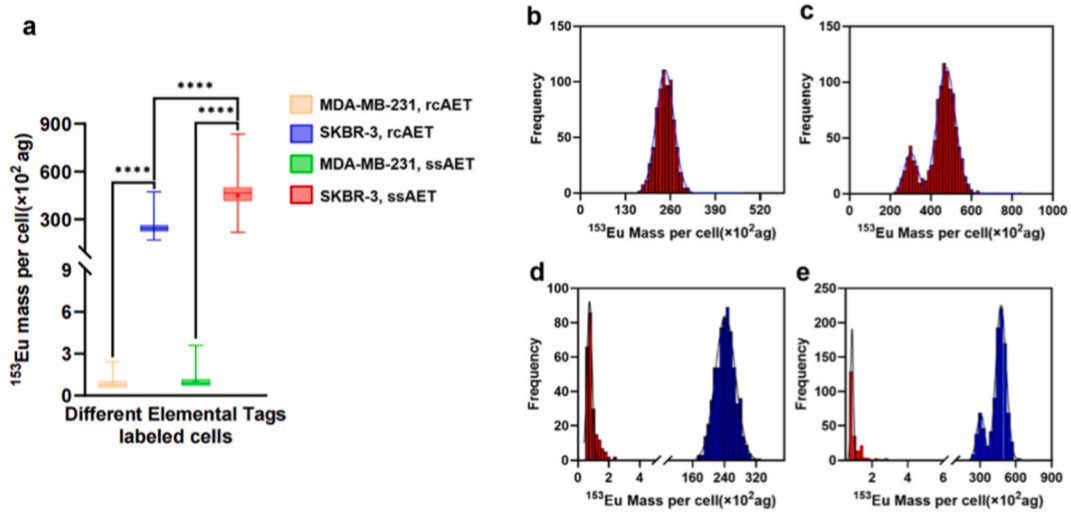

Fig. 3. (a) Box plot corresponding to the comparison of labeling efficiency of SKBR-3 cells using rcAET and ssAET by quantifying the ^{153}Eu mass per cell (SKBR-3 cell), in which the percentile line of the box chart was set at the segments of 0 %, 25 %, 50 %, 75 %, and 100 %; + in the center of the boxes represents the mean value. P-value was calculated by ANOVA test (n = 7). Frequency distribution histograms of ^{153}Eu per cell for rcAET- (b) and ssAET- (c) labeled SK-BR3 cells, demonstrating HER2 receptor heterogeneity on cell surfaces. Processed frequency distribution histograms of rcAET- (d) and ssAET- (e) labeled MDA-MB-231/SK-BR3 cell mixtures after data analysis.

SKBR-3 cells. While rcAET-labeled cells displayed a unimodal Gaussian distribution (Fig. 3b), ssAET-labeled cells showed a bimodal pattern (Fig. 3c), suggesting that ssAET can resolve subpopulations with distinct HER2 expression levels. This observation aligns with the known biological heterogeneity of HER2 expression in breast cancer cells [40,41] and highlights the superior resolving power of ssAET for single-cell heterogeneity analysis.

To validate the feasibility of specifically differentiating the malignant phenotype of HER2 within complex cell populations using antibody-elemental tags constructed based on diverse strategies, initially, MDA-MB-231 and SKBR-3 in optimal growth states were enumerated via cell counting. Subsequently, the two cell types were combined at a 1:1 ratio to formulate a cell mixture, with the overall cell concentration set at 2×10^6 cells/mL. Fig. S15 presents the original signals obtained by SC-ICP-MS, and the corresponding frequency distribution histograms are displayed in Fig. 3d and e. After Gaussian fitting, it was observed that when the cell mixture was labeled with rcAET and ssAET respectively, in addition to the two Gaussian distributions generated by the ssAET-labeled positive cells, two sets of Gaussian distributions appeared in the frequency distribution histogram. Together, these results demonstrate that ssAET not only provides enhanced sensitivity and specificity but also enables detailed profiling of cellular heterogeneity and population structure in complex biological samples.

4. Conclusions

In conclusion, we have successfully constructed ssAETs by introducing an azide moiety selectively into the Fc domain of antibodies through a rapid and traceless binding-induced group transfer reaction. Unlike enzymatic or genetic engineering approaches to antibody labeling, which often require antibody re-design or leave residual linkers/peptides attached, our method is entirely genetic engineering-free and traceless–meaning no extra peptide or linker remains on the antibody after labeling. This yields a truly native antibody structure with a precisely defined 1:1 labeling stoichiometry, an outcome difficult to achieve with earlier methods. Using SC-ICP-MS, we demonstrated that ssAETs exhibit superior uniformity, high specificity, and enhanced sensitivity in detecting HER2-positive cells compared with rcAETs. Moreover, the constructed ssAET features the ability to reveal the heterogeneity of HER2 expression within the SK-BR3 cell population, confirming its unique advantages in complex cells typing and heterogeneity analysis. Beyond HER2 detection, this site-specific tagging platform offers a versatile and robust approach for single-cell biomarker profiling. By employing distinct oligonucleotide sequences with lanthanide-loaded MS2 nanocarriers, it enables simultaneous and quantitative multiplexed labeling of multiple biomarkers, demonstrating broad compatibility with both CyTOF and fast-scanning quadrupole ICP-MS platforms for high-throughput, multi-element single-cell analysis.

CRediT authorship contribution statement

Haowen Hu: Writing – original draft, Investigation, Data curation, Conceptualization. **Zhengxian Lv:** Writing – review & editing, Investigation. **Yixin Guo:** Writing – original draft, Investigation, Data curation. **Li Yi:** Investigation. **Limin Yang:** Writing – review & editing. **Xiaowen Yan:** Writing – review & editing, Supervision, Project administration, Funding acquisition, Conceptualization. **Qiuquan Wang:** Writing – review & editing, Supervision, Resources, Project administration, Funding acquisition.

Notes

The authors declare no competing financial interest.

Declaration of competing interest

The authors declare that they have no known competing financial interests or personal relationships that could have appeared to influence the work reported in this paper.

Acknowledgments

This study was financially supported by the National Key Research and Development Program of China (2022YFF0710200), the National Natural Science Foundation of China (22074127, 22193053, 21874111, 22304050), the Fujian Provincial Natural Science Foundation of China (2025J01017), the Science and Technology Projects of Innovation Laboratory for Sciences and Technologies of Energy Materials of Fujian Province (IKKEM) (HRTP-[2022]-13), and the Fundamental Research Funds for the Central Universities (20720200073).

Appendix A. Supplementary data

Supplementary data to this article can be found online at https://doi.org/10.1016/j.talanta.2025.129227.

Data availability

Data will be made available on request.

References

[1] C. Zhang, F. Wu, Y. Zhang, X. Wang, X. Zhang, A novel combination of immunoreaction and ICP-MS as a hyphenated technique for the determination of thyroid-stimulating hormone (TSH) in human serum, J. Anal. At. Spectrom. 16 (2001) 1393–1396.

[2] R. Lobiński, D. Schaumlöffel, J. Szpunar, Mass spectrometry in bioinorganic analytical chemistry, Mass Spectrom. Rev. 25 (2006) 255–289.

[3] J.S. Becker, N. Jakubowski, The synergy of elemental and biomolecular mass spectrometry: new analytical strategies in life sciences, Chem. Soc. Rev. 38 (2009) 1969–1983.

[4] X. Yan, L. Yang, Q. Wang, Detection and quantification of proteins and cells by use of elemental mass spectrometry: progress and challenges, Anal. Bioanal. Chem. 405 (2013) 5663–5670.

[5] H. Wang, M. He, B. Chen, B. Hu, Advances in ICP-MS-based techniques for trace elements and their species analysis in cells, J. Anal. At. Spectrom. 32 (2017) 1650–1659.

[6] M. Corte-Rodríguez, E. Blanco-González, J. Bettmer, M. Montes-Bayón, Quantitative analysis of transferrin receptor 1 (TfR1) in individual breast cancer cells by means of labeled antibodies and elemental (ICP-MS) detection, Anal. Chem. 91 (2019) 15532–15538.

[7] P. Chang, L. Zheng, B. Wang, M. Chen, M. Wang, J. Wang, W. Feng, ICP-MS-based methodology in metallomics: towards single particle analysis, single cell analysis, and spatial metallomics, At. Spectrosc. 43 (2022) 255–265.

[8] Y. Liang, Z. Liu, D. Zuo, S. Chen, J. Chen, X. Ya, Q. Wang, Single cell glycan-linkages profiling for hepatocellular carcinoma early diagnosis using lanthanide encoded bacteriophage MS2 based ICP-MS, Talanta 274 (2024) 126056.

[9] G. Han, M.H. Spitzer, S.C. Bendall, Metal-isotope-tagged monoclonal antibodies for high-dimensional mass cytometry, Nat. Protoc. 13 (2018) 2121–2148.

[10] J. Hu, X. Yan, Le X. Chris, Label-free detection of biomolecules using inductively coupled plasma mass spectrometry (ICP-MS), Anal. Bioanal. Chem. 416 (2024) 2625–2640.

[11] R. Hou, Y. Gu, Y. Zhao, X. Zhao, L. Yang, X. Yan, Q. Wang, Covalent targeting drug mediated specific lanthanide tagging towards in Situ Bruton's tyrosine kinase quantification using ICP-MS, At. Spectrosc. 45 (2024) 74–82.

[12] Z. Fang, X. Zhao, R. Hou, Y. Zhao, X. Yan, Q. Wang, Antibody-directed cell internalization of targeted covalent europium tag enables in situ kinase labeling and inductively coupled plasma mass spectrometry (ICP-MS) quantification, Anal. Chem. 23 (2025) 12125–12132.

[13] R. Liu, S. Zhang, C. Wei, Z. Xing, S. Zhang, X. Zhang, Metal stable isotope tagging: renaissance of radioimmunoassay for multiplex and absolute quantification of biomolecules, Acc. Chem. Res. 49 (2016) 775–783.

[14] L.P. Arnett, R. Rana, W.W.-Y. Chung, X. Li, M. Abtahi, D. Majonis, J. Bassan, M. Nitz, M.A. Winnik, Reagents for mass cytometry, Chem. Rev. 123 (2023) 1166–1205.

[15] X. Lou, G. Zhang, I. Herrera, R. Kinach, O. Ornatsky, V. Baranov, M. Nitz, M. A. Winnik, Polymer-based elemental tags for sensitive bioassays, Angew. Chem. Int. Ed. 46 (2007) 6111–6114.

[16] A.I. Abdelrahman, S. Dai, S.C. Thicket, O. Ornatsky, D. Bandura, V. Baranov, M. A. Winnik, Lanthanide-containing polymer microspheres by multiple-stage dispersion polymerization for highly multiplexed bioassays, J. Am. Chem. Soc. 131 (2009) 15276–15283.

[17] R. Yuan, F. Ge, Y. Liang, Y. Zhou, L. Yang, Q. Wang, Viruslike element-tagged nanoparticle inductively coupled plasma mass spectrometry signal multiplier: membrane biomarker mediated cell counting, Anal. Chem. 91 (2019) 4948–4952.

[18] Z. Huang, X. Zhao, J. Hu, C. Zhang, X. Xie, R. Liu, Y. Lv, Single-Nanoparticle differential immunoassay for multiplexed gastric cancer biomarker monitoring, Anal. Chem. 94 (2022) 12899–12906.

[19] M. Liu, X. Wei, C. Wu, J. Liu, Y. Wei, X. Wang, J. Wang, Single cell phenotypic analysis for cancer stem cell identification by dual-isotope ICP-QMS, Anal. Chem. 95 (2023) 14447–14454.

[20] X.W. Zhang, M.X. Liu, M.Q. He, S. Chen, Y.L. Yu, J.H. Wang, Integral multielement signals by DNA-programmed UCNP-AuNP nanosatellite assemblies for ultrasensitive ICP–MS detection of exosomal proteins and cancer identification, Anal. Chem. 93 (2021) 6437–6445.

[21] X. Wu, Q. DeGottardi, I.C. Wu, Lanthanide-coordinated semiconducting polymer dots used for flow cytometry and mass cytometry, Angew. Chem. Int. Ed. 56 (2017) 14908–14912.

[22] Y. Chen, G. Wang, P. Wang, J. Liu, H. Shi, J. Zhao, Y. Luo, Metal-Chelatable porphyrinic frameworks for single-cell multiplexing with mass cytometry, Angew. Chem. Int. Ed. 134 (2022) e202208640.

[23] L. Wang, L. Yi, H. Li, S. Chen, L. Yang, X. Yan, Q. Wang, Synthesis and single-cell analysis application of antibody-element-tag based on peptide affinity-mediated site-specific labeling strategy, Chinese J. Anal. Chem. 52 (2024) 1496–1507.

[24] J. Maynard, G. Georgiou, Antibody engineering, Annu. Rev. Biomed. Eng. 2 (2000) 339–376.

[25] K.E. Tiller, P.M. Tessier, Advances in antibody design, Annu. Rev. Biomed. Eng. 17 (2015) 191–216.

[26] A. Sadiki, S.R. Vaidya, M. Abdollahi, et al., Site-specific conjugation of native antibody, Antib. Ther. 3 (2020) 271–284.

[27] D. Torregrosa, G. Grindlay, L. Gras, J. Mora, Immunoassays based on inductively coupled plasma mass spectrometry detection: so far so good, so what? Microchem. J. 166 (2021) 106200.

[28] S. Jeger, K. Zimmermann, A. Blanc, et al., Site-specific and stoichiometric modification of antibodies by bacterial transglutaminase, Angew. Chem. Int. Ed. 49 (2010) 9995–9997.

[29] T.H. Pillow, J. Tien, K.L. Parsons-Reponte, et al., Site-specific trastuzumab maytansinoid antibody–drug conjugates with improved therapeutic activity through linker and antibody engineering, J. Med. Chem. 57 (2014) 7890–7899.

[30] E.S. Zimmerman, T.H. Heibeck, A. Gill, et al., Production of site-specific antibody-drug conjugates using optimized non-natural amino acids in a cell-free expression system, Bioconjug. Chem. 25 (2014) 351–361.

[31] S.J. Walsh, J.D. Bargh, F.M. Dannheim, A.R. Hanby, H. Seki, A.J. Counsell, X. Ou, E. Fowler, N. Ashman, Y. Takada, A. Isidro-Llobet, J.S. Parker, J.S. Carroll, D. R. Spring, Site-selective modification strategies in antibody-drug conjugates, Chem. Soc. Rev. 50 (2021) 1305–1353.

[32] S. Kishimoto, Y. Nakashimada, R. Yokota, T. Hatanaka, M. Adachi, Y. Ito, Site-specific chemical conjugation of antibodies by using affinity peptide for the development of therapeutic antibody format, Bioconjug. Chem. 30 (2019) 698–702.

[33] Y. Zhou, Z. Chen, J. Zeng, D. Yu, B. Zhang, Q. Wang, Direct infusion ICP-q MS of lined-up single-cell using an oil-free passive microfluidic system, Anal. Chem. 92 (2020) 5286–5293.

[34] H.E. Pace, N.J. Rogers, C. Jarolimek, Determining transport efficiency for the purpose of counting and sizing nanoparticles via single particle inductively coupled plasma mass spectrometry, Anal. Chem. 83 (2011) 9361–9369.

[35] G.J.L. Bernardes, M. Steiner, I. Hartmann, Site-specific chemical modification of antibody fragments using traceless cleavable linkers, Nat. Protoc. 8 (2013) 2079–2089.

[36] Y. Zeng, W. Shi, Q. Dong, W. Li, J. Zhang, X. Ren, C. Tang, B. Liu, Y. Song, Y. Wu, X. Diao, H. Zhou, H. Huang, F. Tang, W. Huang, A traceless site-specific conjugation on native antibodies enables efficient one-step payload assembly, Angew. Chem. Int. Ed. Engl. 61 (2022) e202204132.

[37] S. Kim, N. Kim, S.W. Lee, H. Yi, H.S. Lee, Affinity-directed site-specific protein labeling and its application to antibody-drug conjugates, Adv. Sci. 11 (2024) 2306401.

[38] U. von Pawel-Rammingen, B.P. Johansson, L. Björck, IdeS, a novel streptococcal cysteine proteinase with unique specificity for immunoglobulin G, EMBO J. 21 (2002) 1607–1615.

[39] K.G. Heumann, L. Rottmann, J. Vogl, Elemental speciation with liquid chromatography–inductively coupled plasma isotope dilution mass spectrometry, JAAS 9 (1994) 1351–1355.

[40] F. Weinberg, D.B. Peckys, N. Jonge, EGFR expression in HER2-driven breast cancer cells, Int. J. Mol. Sci. 21 (2020) 9008.

[41] Q. Zhu, X. Zhao, Y. Zhang, Y. Li, S. Liu, J. Han, L. Wu, Single cell multi-omics reveal intra-cell-line heterogeneity across human cancer cell lines, Nat. Commun. 14 (2023) 8170.